

Supplemental Information

Phosphatidylcholine Synthesis for Lipid Droplet Expansion Is Mediated by Localized Activation of CTP:Phosphocholine Cytidylyltransferase

Natalie Krahmer, Yi Guo, Florian Wilfling, Maximiliane Hilger, Susanne Lingrell, Klaus Heger, Heather W. Newman, Marc Schmid-Supprian, Dennis E. Vance, Matthias Mann, Robert V. Farese, Jr., and Tobias C. Walther

INVENTORY OF SUPPLEMENTAL INFORMATION

SUPPLEMENTAL FIGURES

Figure S1, Related to Figure 1: Enzymes for PC and PE Synthesis Are Efficiently Knocked Down by RNAi; CCT1 Promoted LD Fusion Is Independent of SNAREs; CCT, CK and SCAP Phenotypes Are Caused by PC Deficiency

Controls and additional primary data for experiments shown in Figure 1.

Figure S2, Related to Figure 3: CCT2 Is Targeted to LDs with a Delay; CK Depletion Increases CCT LD targeting

Analogous experiments as shown in Figure 3 with the CCT1 enzyme homolog CCT2 and additional primary data for Figure 3.

Figure S3, Related to Figure 4: CCT2 Binds Stably to LDs

Analogous experiments as shown in Figure 4 with the CCT1 enzyme homolog CCT2.

Figure S4, Related to Figure 5: CCT Directly Binds to LDs

Additional primary data for Figure 5.

Figure S5, Related to Figure 5: mCherry-CCT1, but Not mCherry-CCT1W397E, Is Activated by Oleate Loading or Artificial Droplets with Low PC. Nucleocytoplasmic Shuttling Is Not Necessary for CCT1 Function during LD Expansion.

Additional experiments for Figure 5.

Figure S6, Related to Figure 6: Mammalian CCT α Localizes to LDs in S2 Cells and in N2a Cells and Is Activated by LD Targeting or PC Deficient Artificial Droplets

Additional data of experiments shown in Figure 6 using another cell type.

Figure S7, Related to Figure 6: HTNC Treatment of BMDM from CCT α ^{fllox} Mice Efficiently Depletes CCT α Expression.

Control experiments for data shown in Figure 6F.

SUPPLEMENTAL MOVIES

Movie S1, Related to Figure 4A, B: Movie of experiments shown in Figure 4A, B

Movie S2, Related to Figure 4 C, D: Movie of experiments shown in Figure 4C, D

Movie S3, Related to Figure 4E, F: Movie of experiments shown Figure 4E, F

Movie S4, Related to Figure 4G, H: Movie of experiments shown Figure 4G, H

SUPPLEMENTAL TABLES

Table S1: Proteomic Analysis of CCT Targeting to LDs.

Gene names, the number of unique peptides, the SILAC ratio indicating purification of the corresponding proteins and the summed intensities for proteins are shown.

Table S2: Sequences of Primers Used for RNAi Experiments.

Table S3: Sequences of Primers Used for Quantitative Reverse Transcription PCR.

SUPPLEMENTAL EXPERIMENTAL PROCEDURES

Protein Binding to Artificial Droplets

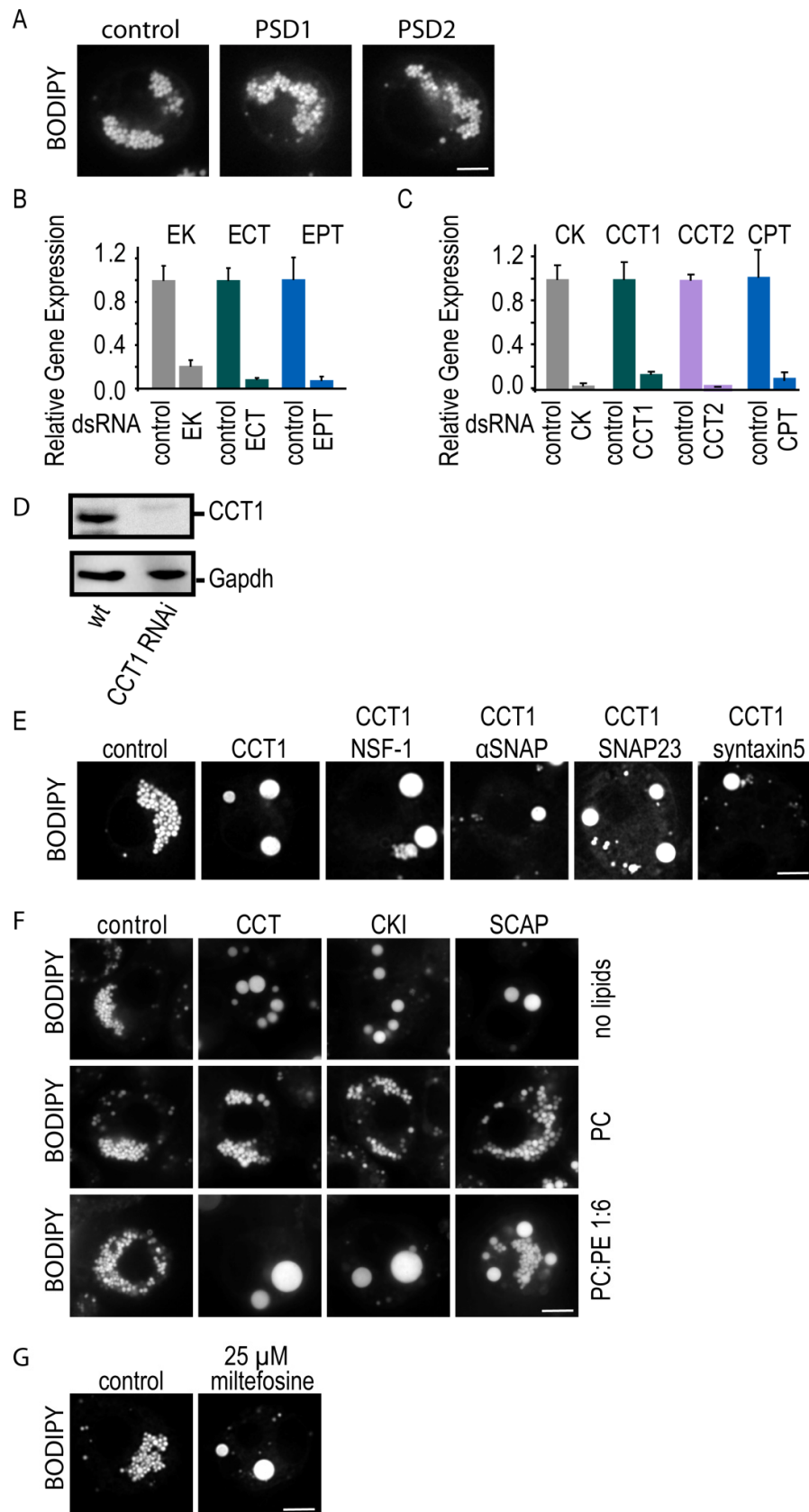
Experimental procedure for Figure S4.

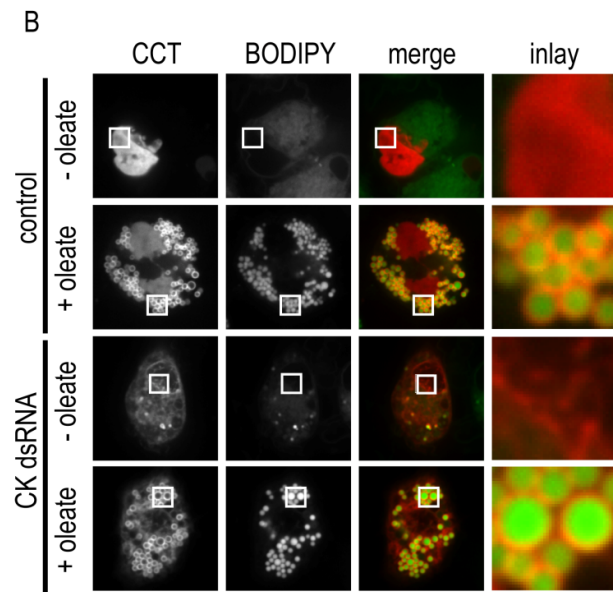
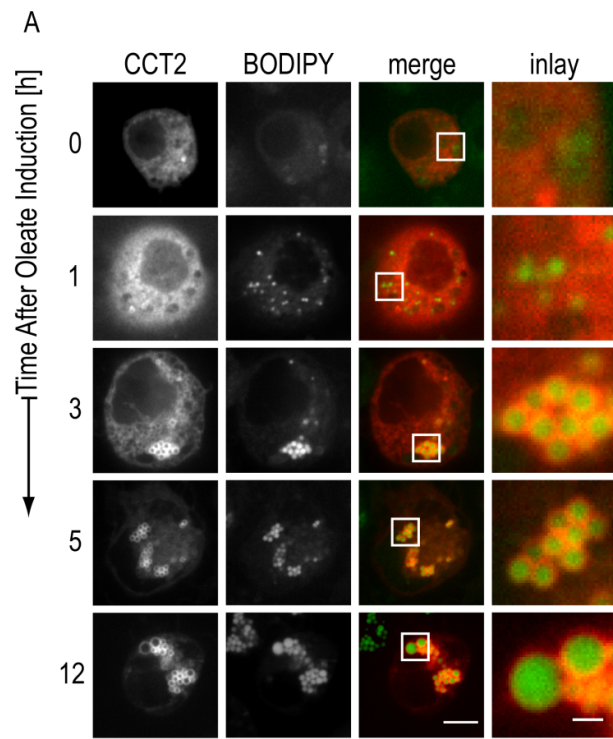
Mass Spectrometry–Based Proteomics

Additional experimental procedures for Figure 2C.

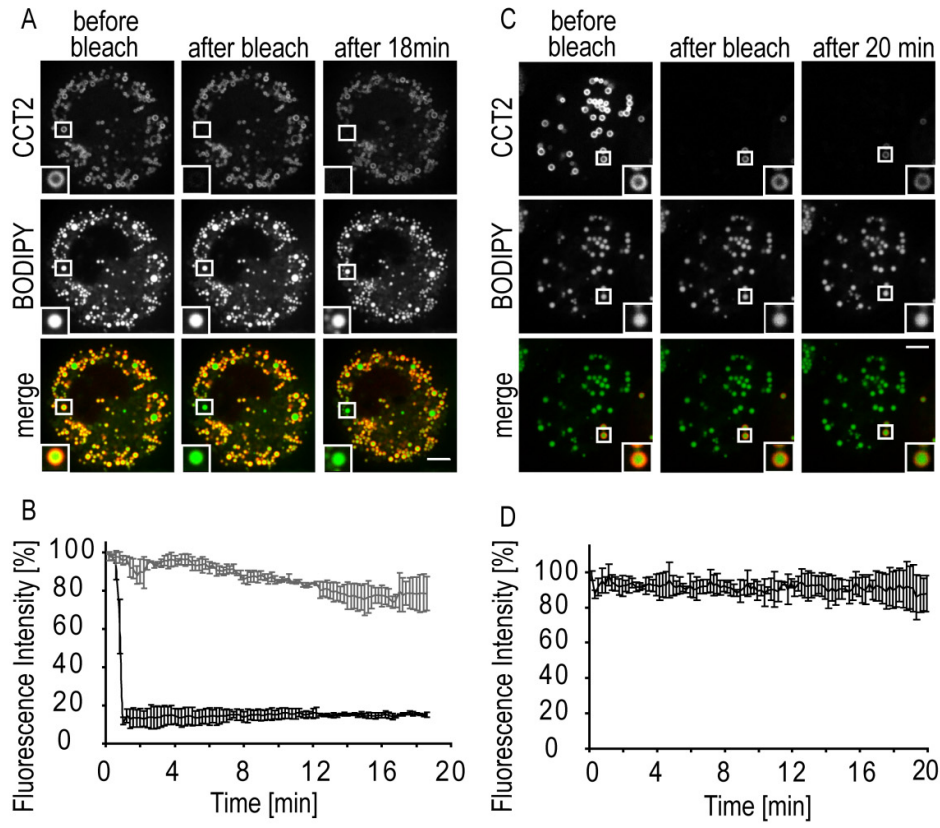
SUPPLEMENTAL REFERENCES

SUPPLEMENTAL FIGURES

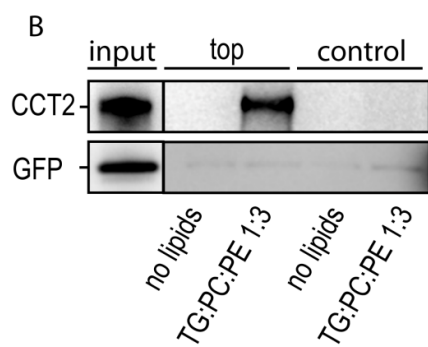
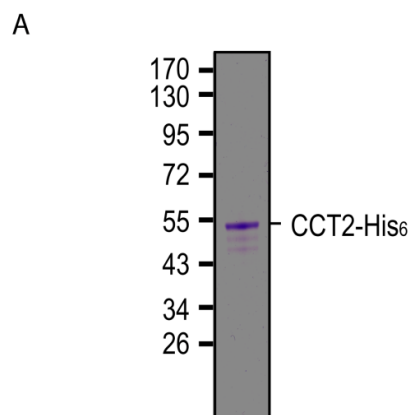




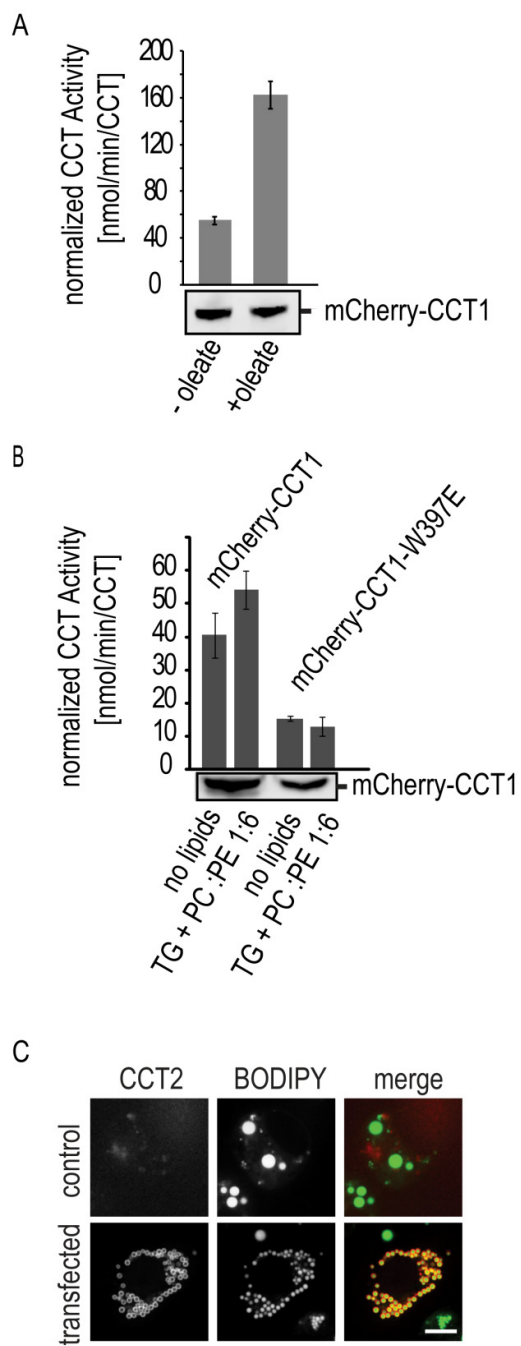
Krahmer et al. Figure S2



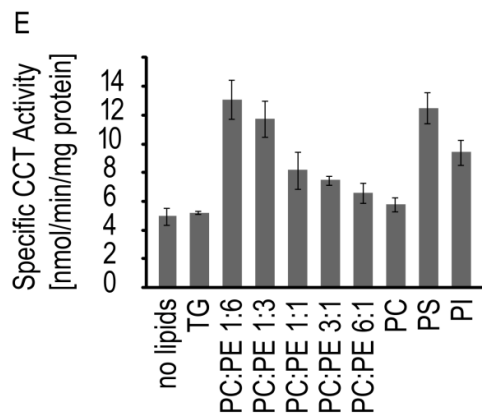
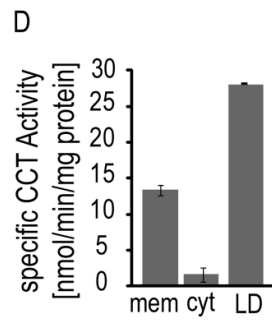
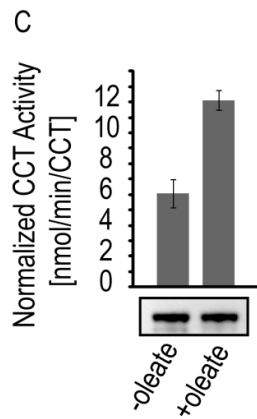
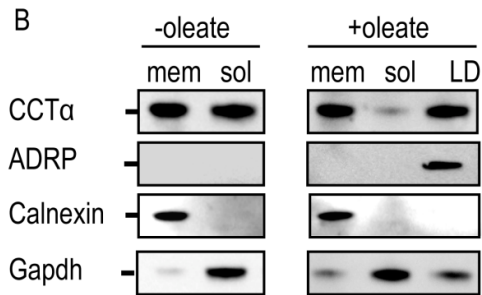
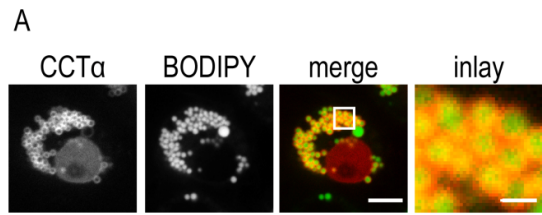
Krahmer et al. Figure S3



Krahmer et al. Figure S4

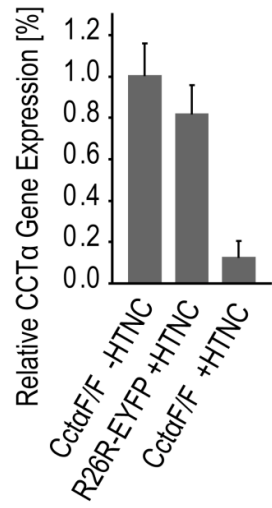


Krahmer et. al Figure S5

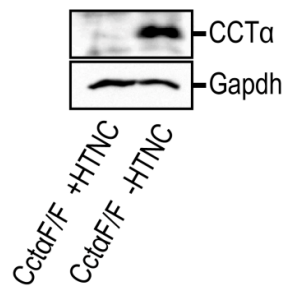


Krahmer et. al Figure S6

A



B



Krahmer et al. Figure S7

SUPPLEMENTAL FIGURE LEGENDS

Figure S1, Related to Figure 1: Enzymes for PC and PE Synthesis Are Efficiently Knocked Down by RNAi; CCT1 Promoted LD Fusion Is Independent of SNAREs; CCT, CK and SCAP Phenotypes Are Caused by PC Deficiency

(A) PSD1 and PSD2 knockdowns do not influence LD morphology. PSD1 and PSD2 depleted and oleate loaded cells were stained with BODIPY. Bar = 5 μ m.

(B and C) Enzymes of the PE and PC synthesis pathways were knocked down with at least 80% efficiency. Expression levels were measured by quantitative Real-Time PCR. Total RNA was prepared with the PrepAse Kit (USB); 3 μ g was used for first-stand cDNA synthesis with a kit (Fermentas). Real-time quantitative PCR was performed with the MyiQ™ Single-Color Real-Time PCR Detection System (BioRad) and Mesa green (Eurogentec). Primers used are listed in Table S3. Values are mean \pm SD of three experiments.

(D) CCT1 protein was completely depleted by RNAi treatment. Western blot shows complete depletion of CCT1 in total lysate of S2 cells treated with dsRNA directed against CCT1, whereas no effect on CCT1 levels was observed in control treated S2 cells. Gapdh was used as a loading control.

(E) CCT1 promoted LD fusion is independent of the SNARE protein machinery. Knockdown of the indicated proteins does not suppress the CCT1 phenotype. Cells depleted of CCT1 and the indicated proteins were oleate loaded and stained with BODIPY. Bar = 5 μ m.

(F) CCT1, CK and SCAP knockdowns can be rescued by addition of PC liposomes but not or only partially by liposomes consisting mainly of PE. *Drosophila* S2 cells treated with RNAi directed against CCT1 were incubated with 5 mM liposomes of the indicated lipid mixtures before LD morphology was analyzed 12 h after oleate treatment. LDs were stained with BODIPY. Bar = 5 μ m.

(G) The CCT inhibitor miltefosine induces the formation of giant LDs. *Drosophila* S2 cells were treated with 25 μ M miltefosine for 48 h and oleate for 12 h. LDs were stained with BODIPY. Bar = 5 μ m.

Figure S2, Related to Figure 3: CCT2 Is Targeted to LDs with a Delay; CK depletion increases CCT LD targeting

(A) Three hours after oleate loading, CCT2 localizes to LDs. mCherry-CCT2 was expressed in S2 cells (left panels). LD targeting was followed after the addition of 1 mM oleate to the medium. LDs were stained with BODIPY (second left panels). Second right panels show overlays of the two channels. Right panel shows a zoom of a representative LD section. Bars = 5 μ m (overview) or 1 μ m (inlay).

(B) PC deficiency caused by CK depletion increases LD targeting of CCT. CCT1 was expressed in CK depleted cells and CCT1 LD targeting was compared to control cells before and after oleate treatment. Cells analyzed as in (A).

Figure S3, Related to Figure 4: CCT2 Binds Stably to LDs

(A) CCT2 fluorescence does not recover on a bleached LD. FLIP of mCherry-CCT2 in *Drosophila* S2 cells treated with oleate for 12 h. CCT2 was tagged with mCherry (upper panel), LDs were stained with BODIPY (middle panels). The lower panels show the overlay of the two channels. The box indicates the LD that was photobleached in the cell. Insets show the indicated part of the image at higher magnification. Prebleach (left), immediately after bleach (middle panels), and postbleach (right) images of the FRAP experiment are shown. Bar = 5 μ m.

(B) Fluorescence intensity of mCherry-CCT2 on the LD shown in (A) at the beginning of the experiment was set to 100% (black line). A LD in an unbleached cell was used as control to monitor photobleaching during the experiment (grey line). Values indicate the mean \pm SD of three independent experiments.

(C) CCT2 fluorescence remains stable on a single LD in a bleached cell. FLIP of mCherry-CCT2 in *Drosophila* S2 cells treated with oleate for 12 h. CCT2 was tagged with mCherry (upper panels). LDs were stained with BODIPY (middle panels). The lower panels show overlays of the two channels. Box indicates the LD that was not photobleached in the cell.

Insets show the indicated part of the image at higher magnification. Prebleach (left), immediately after bleach (middle), and postbleach (right) images of the FRAP experiment. Bar = 5 μm . The fluorescence of the non-bleached LD was subsequently monitored.

(D) Fluorescence intensity of mCherry-CCT2 on the non-bleached droplet in (C) at the beginning of the experiment was set to 100%. Photobleaching during the time course calculated from a unbleached control cell from the same experiment was subtracted. Values indicate the mean \pm SD of three independent experiments.

Figure S4, Related to Figure 5: CCT Directly Binds to LDs

(A) CCT2-His₆ was affinity purified to high purity. Purity was checked by SDS gel.

(B) CCT2 directly binds to artificial droplets. Purified CCT2-His₆ and a purified GFP control proteins were mixed in a 1:1 ratio and incubated with artificial droplets (phospholipid composition PE:PC 3:1), adjusted to 0.75 M sucrose and floated by centrifugation. The top fraction and a control fraction under the LDs were analyzed by western blot and compared to control samples without lipids.

Figure S5, Related to Figure 5: mCherry-CCT1, but Not mCherry-CCT1W397E, Is Activated by Oleate Loading or Artificial Droplets with Low PC. Nucleocytoplasmic Shuttling Is Not Necessary for CCT1 Function during LD Expansion

(A) mCherry-CCT1 activity increases when cells are loaded with oleate. mCherry-CCT1 activity was measured and normalized as described in Figure 5A. Endogenous CCT activity was measured and subtracted before and after oleate loading. Values indicate the mean \pm SD of three independent experiments.

(B) mCherry-CCT1, but not mCherry-CCT1W397E, is activated by artificial droplets with low PC. Artificial droplets containing PC and PE in a 1:6 ratio were generated and added to total mCherry-CCT1 and mCherry-CCT1W397E cell lysates and the CCT activity was determined. Values indicate the mean \pm SD of three independent experiments.

(C) mCherry-CCT2 (lower left panel) was transiently expressed in cells with endogenous CCT1 knocked down by RNAi against its 3'-UTR and the ability of CCT2 to rescue the LD phenotype was tested in oleate loaded cells. An untransfected control cell of the same sample is shown in the upper panel. LDs were stained with BODIPY (middle panels). The left panels show overlays of the two channels. Bar = 5 μm .

Figure S6, Related to Figure 6: Mammalian CCT α Localizes to LDs in S2 Cells and in N2a Cells and Is Activated by LD targeting or PC Deficient Artificial Droplets

(A) Murine mCherry-CCT α was transiently expressed in S2 cells (left panel), which were loaded with 1 mM oleate for 12 h. LDs were stained with BODIPY (middle panel). The overlays of the two channels and zoom of a representative LD section are shown (right two panels). Bar = 5 μm (overview) or 1 μm (inlay).

(B) Same protein amount of the indicated cellular fractions was blotted against CCT α , ADRP, calnexin and, Gapdh.

(C) Oleate loading increases CCT α activity in N2a cells by. CCT activity was measured in total cell lysate before and after 12h of oleate loading and normalized to enzyme levels measured by western blot. Lower panels show a representative blot of CCT1 expression in samples used for activity assays (equal amounts were loaded onto the blot and in activity assay). Values are mean \pm SD of three independent experiments.

(D) In oleate-loaded cells CCT α activity is highest in the LD fraction. The specific CCT activity was measured for the indicated fractions purified from N2a cells after oleate loading. Values indicate the mean \pm SD of three independent experiments.

(E) Mammalian CCT activity inversely correlates with the PC content of *in vitro* generated artificial droplets. Artificial droplets of the indicated phospholipid compositions were generated, added to total N2a cell lysate, and CCT activity was determined. Values indicate the mean \pm SD of three experiments.

Figure S7, Related to Figure 6: HTNC Treatment of BMDM from CCT α ^{flox} Mice Efficiently Depletes CCT α Expression

(A) CCT α mRNA levels from HTNC-treated BMDMs from *Ccta*^{F/F} mice were monitored by quantitative reverse-transcription PCR and compared to CCT α mRNA levels in untreated BMDM from *Ccta*^{F/F} mice and HTNC-treated BMDM from R26R-eYFP mice. Values indicate the mean \pm SD of three experiments.

(B) CCT α protein was completely depleted in HTNC-treated BMDMs from *Ccta*^{F/F} mice. Western blot shows complete depletion of CCT α in total cell lysate from HTNC-treated BMDMs from *Ccta*^{F/F} mice. Gapdh was used as a loading control.

SUPPLEMENTAL MOVIES

Movie S1, Related to Figure 4A, B. Movie of FLIP experiment. The signal of mCherry-CCT1 was bleached at the indicated point in the cytosol.

Movie S2, Related to Figure 4C, D. Movie of FLIP experiment. The signal of mCherry-CCT1 was bleached at the indicated point in the nucleus.

Movie S3, Related to Figures 4E, F. Movie of FRAP experiment. The signal of mCherry-CCT1 was bleached at the indicated LD.

Movie S4, Related to Figures 4G, H. Movie of iFRAP experiment. The signal of mCherry-CCT1 was bleached throughout the cell. Only the signal of the indicated LD was left.

SUPPLEMENTAL TABLES

Protein	Unique Peptides	Ratio H/L S1	Ratio H/L S2	Ratio H/L S3	Ratio H/L S4	Ratio H/L S5	Ratio H/L S6	Ratio H/L S7	Ratio H/L S8	Ratio H/L S9
CCT	25	1.7473	0.4621	0.6541	0.0837	0.0344	0.0232	0.2051	0.0706	0.2986
PDI	59	1.9866	0.9999	1.1652	2.1138	1.3160	1.0290	1.1985	3.0081	2.8824
HSL	25	1.0205	0.1654	0.1404	0.0356	0.0575	0.0324	0.0607	0.0259	0.0428
CoVa	8	3.1647	0.6766	0.9095	0.3873	0.1415	0.1103	2.6030	6.4812	10.1150
Lamin	33	2.0819	1.8889	0.8685	0.5119	0.3661	0.2537	0.8504	1.4770	9.3600
ALDH	25	2.0152	2.2635	9.3392	12.9160	15.7490	13.6390	6.8205	3.6061	10.2060

Table S1. Proteomic Analysis of CCT Targeting to LDs.

Gene names, the number of unique peptides and the SILAC ratio (indicating purification) are shown.

Gene	Gene ID	Forward	Reverse
CCT1	CG1049	ACA TCT ATG CTC CTC TCA AGG C	CTC TGC AGA CTC TGG TAA CTG C
CCT1-3'UTR	CG1049	ATG ACA TAC CCT ATG GAG CTG G	ATATTGGTTGGTGTCTGGTTGCG
CCT2	CG18830	ATG ACA TAC CCT ATG GAG CTG G	TGT TTT CGA CTA AGG GAT ACG C
CK	CG2201	TGG ACA CTA CGA ATG ACT CAG C	ACA TTA ATT ACG GAC CAA AGG C
CPT	CG7149	GTT CTC TTC ATC TTT TGG GG C	AAT GAG CCT CCG ACA AGT AGC
EK	CG3525	CTC GAA AGG TGG AGT TTT TGT C	AAG TAC ATA CCT TCG CTT TAT TAT GAC
ECT	CG5547	GTC TTG TTT AGT ATG TCG TCC CC	TTG GAA TTC GCA ATA TTT TTG G
EPT	CG6016	GAT GGA GTA TCT GGA CTG GTC G	GAC TGC AAC AGT TCT GTC TCC C
pBluescript		AATTCGATATCAAGCTTATCGAT	TAAATTGTAAGCGTTAATATTTTG
PSD1	CG5991	TGATGTTAATTTGAGCGAGGC	TTTGTTCAGACCAGTTCATCG
PSD2	CG12576	CGGATTCAAATCGAGATCGT	ACTGGGAAAACCTTTTGGCT
αSNAP	CG6625	TAGAGGAACAGAACATCGAGGG	GAAATTCATTTTCGCTACCAGG
SNAP23	CG40452	CAAACGGTCCTCATGGTTT	GCGACAATCAGCAAAGAACA
syntaxin5	CG4214	TGTTTAGGACACACAAACCTGC	ATGACGAATATTTCTGGTTCGG
NSF	CG33101	GGTGTCTGTTCTCATCGAAGG	CCACTCTGCTGTTTGATAATGG
SCAP	CG33131	CACTAAGTGGGCACTACGTTACC	GAAGTAGTCAAGGCACCAGACC

Table S2: Sequences of Primers Used for RNAi Experiments.

Gene	Gene ID	Forward	Reverse
<i>CCT1</i>	CG1049	GGA AGC GGA CCT ACG AGA TA	GTG CCC TGA TCC TGA ACT T
<i>CCT2</i>	CG18830	GAT GAG ATC GTT CCG AAT GC	CAC AAA CAT TCC CTT CGC TT
<i>CK</i>	CG2201	CGG GAG TCA ATC AGT AGC CT	CGT GAT TTG TGT GTC TCC GT
<i>CPT</i>	CG7149	AAA TAT TGC ATG CCG ACT GA	TCT GAG TCG AAG ACC TGC TG
<i>EK</i>	CG3525	CCG GAG GAT AAA TCC AGA AA	ACC TTC AAC AGT TCC TTG GC
<i>ECT</i>	CG5547	GTG GGT CAC CTG GAC TTT CT	GTA GGA GTT CAC CAC GGG AT
<i>EPT</i>	CG6016	ATC CCA ACT GGC TGT TCT TC	CGA AAC CAA ATG AAT GGC TA
<i>Gapdh</i>	CG83393	ATG AAG GTG GTC TCC AAC GC	TCA TCA GAC CCT CGA CGA
<i>CCTα</i>	Pcyt1a, NM_001163160	TTG TGC AGA AGG TGG AAG AG	CAT GTG CTT CAG TGC TCC TT
<i>beta actin</i>	Actb, NM_007393	GGT CAT CAC TAT TGG CAA CG	TCC ATA CCC AAG GAA GG

Table S3: Sequences of Primers Used for Quantitative Reverse Transcription PCR Experiments.

SUPPLEMENTAL EXPERIMENTAL PROCEDURES

Cell Culture

Drosophila S2 cells were cultured, transfected, and treated with oleate and RNAi as described (Guo et al., 2008). A list of primers to generate dsRNAs for RNAi experiments is given in Table S2. A segment of pBluescript backbone was used as the template for control RNAi. For protein localization in S2 cells, we cloned mCherry-CK (CG2201), mCherry-CCT1(CG1049), mCherry-CCT1 Δ P (amino acids (aa) 1–433), mCherry-CCT1 Δ MP (aa 1–365), mCherry-CCT1 M (aa 365–429), mCherry-CCT2 (CG18330) and mCherry-CPT (CG7149) expression vectors (actin promoter) with the Gateway system (Invitrogen). mCherry-CCT1W397E was generated by QuickChange II mutagenesis (Stratagene). S2 cells were transfected with Effectene (Qiagen) according to manufacturer's instructions.

For choline deficiency and SILAC labeling, we grew S2 cells in custom Schneider medium (Bonaldi et al., 2008), with or without 1 mM choline, or 0.4 g/l $^{13}\text{C}_6^{15}\text{N}_4$ L-arginine and 1.65 g/l $^{13}\text{C}_6^{15}\text{N}_2$ L-lysine (Sigma Isotec), respectively.

Raw 264.7 cells (American Type Culture Collection) were cultured in RPMI (Biochrom) with 10% fetal bovine serum and 100 unit/ml penicillin and 100 $\mu\text{g}/\text{ml}$ streptomycin in uncoated dishes at 37°C and transfected with Lipofectamine 2000 (Invitrogen). CCT α -GFP was provided by Dr. Neale Ridgway. N2a cells (American Type Culture Collection) were cultured and differentiated with 1 mM dibutyryl cyclic AMP as described (Tremblay et al., 2010).

CCT α -deficient BMDMs macrophages from *Ccta*^{FF} mice (Jackson Laboratory) and R26R-EYFP mice (Srinivas et al., 2001) were generated as described (Granucci et al., 2001). For Tat-Cre (HTNC) treatment, 5 x 10⁶ cells were plated in 10-cm untreated cell culture plates, washed three times with phosphate-buffered saline (PBS), and incubated for 1 h at 37°C in 5 ml of serum-free medium (Hyclone) containing 1 μM recombinant HTNC [expressed and purified as described (Peitz et al., 2007)], 200 μM chloroquin (Sigma), 50 $\mu\text{g}/\text{ml}$ polymyxin (Calbiochem), and 2 μM leupeptin (Sigma). Five days later, cells were incubated with 1 mM oleate for 24 h and imaged. To quantify BMDM purity and HTNC recombination efficiency, cells were stained with PE-labeled anti-CD11b antibody (eBioscience) and analyzed for EYFP expression by flow cytometry (FACSCalibur, BD).

Protein Binding to Artificial Droplets

CCT2-His₆ (100 μM), expressed and affinity purified as described (Helmink and Friesen, 2004), was incubated with artificial droplets (2.5 mM phospholipids and 1 mM TG) in a 1 ml reaction for 1 h on ice in buffer (150 mM NaCl, 50 mM Tris/HCl, pH 7.5, 1 mM EDTA). The reaction mix was adjusted to 0.75 M sucrose, overlaid with 10 ml of buffer, and artificial droplets were floated for 1 h at 100,000g. The top fraction was collected with a tube slicer, and an adjacent control fraction was taken under the floating lipid fraction.

Mass Spectrometry–Based Proteomics

Proteomics experiments were performed as described (Hilger et al., 2009). Spectra were analyzed with MaxQuant (version 1.1.0.17) (Cox and Mann, 2008). Precursor and fragment ions were searched with a maximal initial mass deviation of up to 7 ppm and 0.5 Da, respectively. Maximally, two missed cleavages and three labeled amino acids were allowed. A false discovery rate of 0.01 was required for proteins and peptides with a minimum length of 6 amino acids. Summed intensities, SILAC ratios, and the number of unique peptides identified are listed in Table S1.

SUPPLEMENTAL REFERENCES

Bonaldi, T., Straub, T., Cox, J., Kumar, C., Becker, P.B., and Mann, M. (2008). Combined use of RNAi and quantitative proteomics to study gene function in *Drosophila*. *Mol. Cell* *31*, 762–772.

Cox, J., and Mann, M. (2008). MaxQuant enables high peptide identification rates, individualized p.p.b.-range mass accuracies and proteome-wide protein quantification. *Nat Biotechnol* *26*, 1367-1372

Granucci, F., Vizzardelli, C., Pavelka, N., Feau, S., Persico, M., Virzi, E., Rescigno, M., Moro, G., and Ricciardi-Castagnoli, P. (2001). Inducible IL-2 production by dendritic cells revealed by global gene expression analysis. *Nat. Immunol.* *2*, 882–888.

Hilger, M., Bonaldi, T., Gnad, F., and Mann, M. (2009). Systems-wide analysis of a phosphatase knock-down by quantitative proteomics and phosphoproteomics. *Mol Cell Proteomics* *8*, 1908-1920.

Srinivas, S., Watanabe, T., Lin, C.S., William, C.M., Tanabe, Y., Jessell, T.M., and Costantini, F. (2001). Cre reporter strains produced by targeted insertion of EYFP and ECFP into the ROSA26 locus. *BMC Dev. Biol.* *1*, 4.

Tremblay, R.G., Sikorska, M., Sandhu, J.K., Lanthier, P., Ribocco-Lutkiewicz, M., and Bani-Yaghoub, M. (2010). Differentiation of mouse Neuro 2A cells into dopamine neurons. *J. Neurosci. Methods* *186*, 60–67.